polymers

Article

Synthesis of High Performance Cyclic Olefin Polymers (COPs) with Ester Group via Ring-Opening Metathesis Polymerization

Jing Cui [1], Ji-Xing Yang [1], Yan-Guo Li [2,*] and Yue-Sheng Li [1,*]

[1] School of Material Science and Engineering, Tianjin University, Tianjin 300072, China;
E-Mails: cuijing@tju.edu.cn (J.C.); jxyang@ciac.ac.cn (J.-X.Y.)

[2] Changchun Institute of Applied Chemistry, Chinese Academy of Sciences, Changchun 130022, China

* Authors to whom correspondence should be addressed; E-Mails: liyg@ciac.jl.cn (Y.-G.L.);
ysli@tju.edu.cn (Y.-S.L.); Tel./Fax: +86-22-2740-4377 (Y.-S.L.).

**Abstract:** Novel ester group functionalized cyclic olefin polymers (COPs) with high glass transition temperature, high transparency, good mechanical performance and excellent film forming ability have been achieved in this work via efficient ring-opening metathesis copolymerization of *exo*-1,4,4a,9,9a,10-hexahydro-9,10(1′,2′)-benzeno-l,4-methanoanthracene (HBM) and comonomers (5-norbornene-2-yl methylacetate (NMA), 5-norbornene-2-yl methyl 2-ethylhexanoate (NME) or 5-norbornene-2-yl methyldodecanoate (NMD)) utilizing the Grubbs first generation catalyst, $Ru(CHPh)(Cl)_2(PCy_3)_2$ (Cy = cyclohexyl, **G1**), followed by hydrogenation of double bonds in the main chain. The fully hydrogenated copolymers were characterized by nuclear magnetic resonance, FT-IR spectroscopy analysis, gel permeation chromatography, and thermo gravimetric analysis. Differential scanning calorimetry curves showed that the glass transition temperatures (T_g) linearly decreased with the increasing of comonomers content, which was easily controlled by changing feed ratios of HBM and comonomers. Static water contact angles tests indicate that hydrophilicity of copolymers can also be modulated by changing the comonomers incorporation. Additionally, the mechanical performances of copolymers were also investigated.

1. Introduction

Cyclic olefin copolymers (COCs) and cyclic olefin polymers (COPs) are very attractive thermoplastic resins with potential enhanced properties such as outstanding transparency, good heat resistance, low moisture absorption, good chemical resistance, and low double refraction [1–3]. Based on performance characteristics, the applications of COCs and COPs have now been extended to production of optical parts for digital cameras and laser beam printers, medical products, and electrical insulation [1,4]. As shown in Scheme 1, COCs are obtained through copolymerization of cycloolefin with ethylene or α-olefin [5–14], and commercialized under the trade names APEL® by Mitsui and TOPAS® by TOPAS advanced polymers (TAP: formerly Ticona and Hoechst) [15,16]. COPs are prepared via ring-opening metathesis polymerization (ROMP) of cycloolefin followed by hydrogenation [17–24], and commercialized under the trade names Zeonex® and Zeonor® by Zeon [25] and Arton® by Japan Synthetic Rubber (JSR) [20,21].
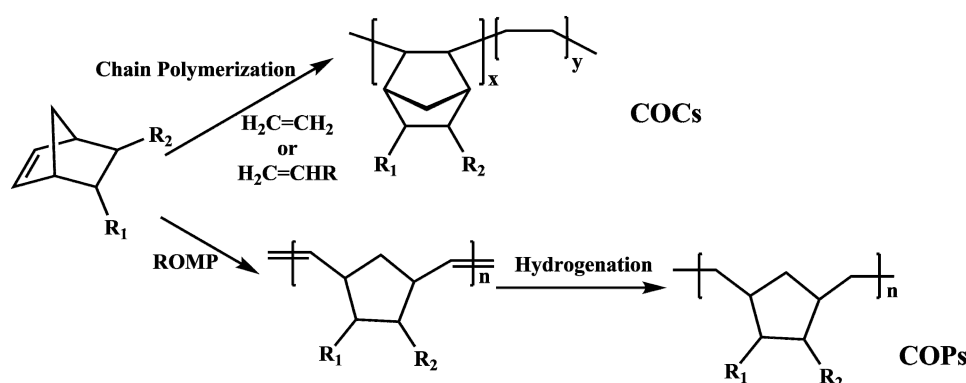

Scheme 1. Typical polymerization routes for COCs (Cyclic olefin copolymers) and COPs (cyclic olefin polymers).

For some applications of COCs and COPs, high T_g is a requirement for keeping good dimensional stability under higher temperature [15,26,27]. The T_g of COCs can be enhanced by increasing the cycloolefin content in the polymer chains [16,28]. Another approach to improve the T_g of COCs is employing a bulkier cycloolefin monomer [15,27,29,30]. Due to its steric effect, high T_g can be achieved at relatively low comonomer incorporation. For instances, we have prepared a novel COC with high T_g (207.0 °C) by copolymerizing a bulky monomer, *exo*-1,4,4a,9,9a,10-hexahydro-9,10(1′,2′)-benzeno-l,4-methanoanthracene (HBM), with ethylene in which HBM content is only 30.4 mol% (**1** in Scheme 2) [31]. For COPs, which can be viewed conceptually as an alternating copolymer of ethene and a cyclic monomer, a sterically hindered cycloolefin seems the only way to improve their T_g [4]. Recently, we have obtained a novel COP by ROMP of HBM and subsequent hydrogenation (**2** in Scheme 2) with high T_g value of about 220 °C [32,33]. The T_g can be adjusted at an attractive region of 160–220 °C via copolymerization of HBM with less bulky monomer (**3** in Scheme 2). It was found that the T_g of the resulted COPs linearly increased with HBM content, which is easily controlled by changing feed ratios.

It is noteworthy that the most COCs and COPs are hydrophobic, which may limit some of their end uses [3,34]. Effective improvement of the material performances, such as toughness, adhesion, paintability, and compatibility with other polymers, can be achieved by introducing some functional

groups into polymer chains [35]. For example, Arton® (**4** in Scheme 2), commercialized by JSR, is a cyclic olefin resin with a polar group in its molecular chain and is good in adhesion, adherence, and miscibility. Direct coordination (co)polymerization of monomers with polar functional groups is very difficult for COCs because of catalysts poisoning. Generally, polar monomer needs to be protected by pre-reaction with protective groups to avoid catalyst deactivation.
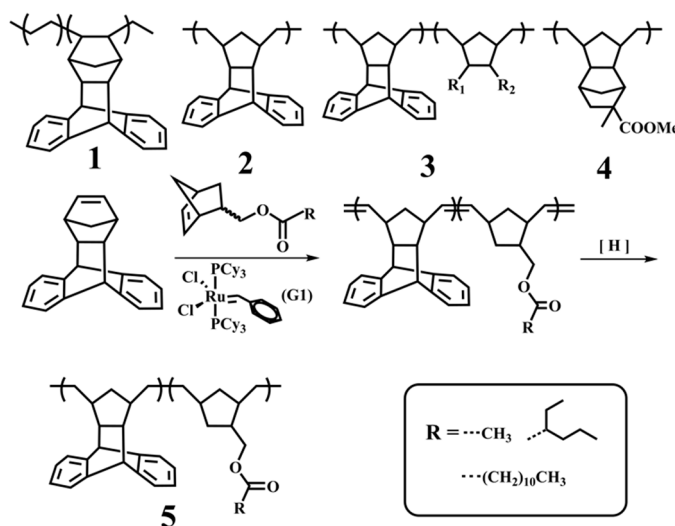
Scheme 2. Structures of COPs in previous reports and the synthetic routes in this work.

Recently, Shiono and his co-workers introduced carbonyl or hydroxyl groups into copolymers via copolymerization of norbornene with ω-alkenylaluminum as a polar monomer precursor [35,36]. Ru-mediated ROMP, nevertheless, has good tolerance towards various functional groups, which allows for the facile introduction of many different functional groups into COPs [37–41]. In this work, we described the synthesis of high-performance functional COPs containing ester groups by copolymerization of HBM with three different comonomers using the Grubbs first generation catalyst, $RuCl_2(PCy_3)_2(CHPh)$ (Cy = cyclohexyl) (**G1**), and subsequent hydrogenation (**5** in Scheme 2).

2. Experimental Section

2.1. General

2.1.1. Procedure and Materials

All manipulation of air- and/or moisture-sensitive compounds were carried out by using standard schlenk techniques or in an MBraun glovebox (MBraun, Munich, Germany) unless otherwise noted under a dry argon atmosphere. All solvents were purified from MBraun solvent purification system (SPS, MBraun, Munich, Germany). *Exo*-1,4,4a,9,9a,10-hexahydro-9,10(1′,2′)-benzeno-l,4-methanoanthracene (HBM) were synthesized according to our previous reports [31,32]. Tetrachloroethane was dried over CaH_2 and distilled before use. 4-Methylbenzenesulfonhydrazide, tripropylamine and butylated hydroxytoluene were purchased from Acros Organic (Themo Fisher Scientific, Fair Lawn, NJ, USA). The **G1** was synthesized according to the method reported previously [42,43]. Ethyl vinyl ether (Stabilized with 0.1% *N,N*-diethyl aniline) was used as received from Alfa Aesar (Karlsruhe, Germany).

2.1.2. Characterization

The NMR data of the monomer and polymer samples were obtained on a Bruker400 MHz spectrometer (400 MHz for ^{1}H, 100 MHz for ^{13}C, Bruker, Karlsruhe, Germany) at ambient temperature, with CDCl$_3$ or CD$_2$Cl$_2$ as a solvent. Chemical shifts (δ) are reported in parts per million relative to the internal standard tetramethylsilane (TMS, δ = 0.00 ppm). Infrared spectra were acquired on a Jasco FT/IR-410 spectrometer (Jasco, Tokyo, Japan); wave numbers in cm^{-1} were reported for characteristic peaks. Differential scanning calorimetry (DSC) measurements were carried out under nitrogen atmosphere at a heating rate of 10 °C/min with a DSC1 Stare System (Mettler Toledo Instruments, Zurich, Swiss) calorimeter up to a temperature of 250 °C using a sample mass in the range of 5–10 mg. The glass transition temperature (T_g), was taken from the second heating scan and was recorded as the midpoint of the step change in heat capacity. The molecular weights and the molecular weight distributions of the polymer samples were determined at 35 °C by a waters 1525 type gel permeation chromatography (GPC). Polymer solutions for GPC tests were prepared with a concentration of *ca.* 0.1% *w/v* in HPLC grade THF, and the calibration was made by polystyrene standard Easi-Cal PS-1 (PL Ltd., Agilen, Santa Clara, California, USA). Thermo gravimetric analyses (TGA) were performed on a Perkin–Elmer Pyris 1 (PerkinElmer Inc., Waltham, Massachusetts, USA) at a heating rate of 10 °C/min in nitrogen or air. The weights of the samples were of about 8 mg. Tensile tests were performed on an 8.9 kN, screw driven universal testing machine (Instron 1211, Canton, Boston, MA, USA) equipped with a 10 kN electronic load cell and mechanical grips. The tests were conducted at room temperature using a cross-head rate of 5 mm/min according to the ASTM standard. The data reported were the mean and standard deviation from at least ten determinations. The static water contact angles (WCA) on the surfaces of COPs films was measured at room temperature and 60% relative humidity using a contact angle goniometer (DSA, KRUSS GmbH, Bremen, Germany) by the sessile drop method with a 3 μL water droplet. The WCA values were recorded after 3 s from droplet deposition. For each value reported, at least five measurements taken from different surface locations were averaged. The angle measure was accurate to ±3. The transparency of copolymer film was recorded on a Shimadzu UV-3600 spectrophotometer (Shimadzu, Kyoto, Japan). X-ray photoelectron spectroscopy (XPS) was used to analyze the surface oxygen atomic state of copolymers with Mono X-Rource (Thermal ESCALAB 250, Thermo Fisher Scientific, Fair Lawn, NJ, USA).

2.2. Ring-Opening Metathesis (Co)polymerization and Hydrogenation Procedure

The mixtures of HBM and comonomer (total weight: 1.5 g) were dissolved in 25 mL dichloromethane (DCM) in a 60 mL glass reactor equipped with a mechanical stirrer at room temperature. Under nitrogen atmosphere, an appropriate amount of **G1** ([monomers]/[**G1**]: 300/1), dissolved in 5 mL dichloromethane, was transferred into the reactor. The mixture was stirred for two hours, until the color changed from purple to red-orange. Excess ethyl vinyl ether was added and the reaction was allowed to stir for 30 min at room temperature. The residue was then precipitated by drop-wise addition of the reaction mixture into vigorously stirred methanol. The polymers were washed three times with methanol and dried in a vacuum oven overnight at 40 °C.

In a typical procedure, unsaturated polymer (1.0 eqv.), 4-methylbenzenesulfonhydrazide (5.0 eqv.), tripropylamine (5.5 eqv.) and a small amount of butylated hydroxytoluene were transferred into a 250 mL round-bottom flask. The mixture was thoroughly degassed and stirred under a nitrogen atmosphere. Then, 30 mL toluene was injected into round-bottom flask and the mixture was refluxed at 110 °C with vigorous stirring. After approximately 16 h, the solution was poured into 150 mL of stirring methanol to yield a white solid. The solid was filtered and washed with distilled water, and then the polymer was redissolved in 20 mL of hot toluene and poured into 150 mL of methanol. This procedure was repeated twice again in order to remove impurities and inorganic substances. The obtained white polymer was dried under vacuum at 50 °C for 24 h. The yields of all the saturated polymers were higher than 85%. The ^{1}H NMR spectra for the homopolymer have been reported [32], and copolymers were provided in Figures 1A and A1 (in Appendix).

2.3. Preparation of Film

The resultant polymer (adjusted to fit a total concentration of 8–10 wt%) was suspended in tetrachloroethane in a 50 mL round-bottom flask, and the mixture was heated at 60 °C for at least 10 h. After the complete dissolution, the thick solution was filtered using a filter. The obtained solution was spread on a glass plate in an oven with a nitrogen atmosphere. The solvent in the spread film was carefully evaporated at 55 °C for 12 h. Then the film was further dried at 60 °C for about 12 h. After the evaporation, the thickness of obtained film was measured about 80–140 μm.

3. Results and Discussion

3.1. HBM/Comonomer Copolymerization

To obtain COPs with improved performances, such as adjustable T_g and hydrophilicity, we have designed and synthesized three norbornene derivatives with ester group as comonomers, 5-norbornene-2-yl methylacetate (NMA), 5-norbornene-2-yl methyl 2-ethylhexanoate (NME) and 5-norbornene-2-yl methyldodecanoate (NMD). Calculated from ^{1}H NMR spectra, it was found that all the comonomers were a mixture of *endo/exo*-isomer with mole ratio of 2:1. A series of ROMP at different HBM/comonomer molar ratios were then carried out using the Grubbs first generation catalyst $Ru(CHPh)(Cl)_2(PCy_3)_2$ (Cy = cyclohexyl, **G1**), which exhibited very high activity to produce well-defined polymers. All the copolymerizations took place efficiently, affording copolymers in quantitative yields. Thus, copolymer compositions can be adjusted precisely and easily by varying the molar ratio of HBM to comonomers (NMA, NME and NMD) in the copolymerization reaction. The typical data including the molecular weights (M_Ws) and molecular weight distributions (M_WDs) of the resultant COPs are summarized in Table 1. All these copolymers showed high M_W, ranging from 40 kg/mol to 110 kg/mol, and relatively narrow M_WDs with polydispersity index (*PDI*) values from 1.24 to 1.60.

Table 1. ROMP (ring-opening metathesis polymerization) of HBM with comonomers by Catalyst **G1** [a].

Run	[HBM]:[M] [b]	HBM (mol%) [c]	Before Hydrogenation [d]		After Hydrogenation [d]	
			M_n (10⁴)	*PDI*	M_n (10⁴)	*PDI*
1	HBM/–	100	9.2	1.29	9.1	1.29
2	HBM/NMA (90:10)	90.8	5.3	1.53	5.7	1.48
3	HBM/NMA (80:20)	81.8	8.0	1.54	9.8	1.45
4	HBM/NMA (70:30)	72.5	4.3	1.60	5.0	1.56
5	HBM/NMA (60:40)	62.5	11.1	1.24	9.7	1.29
6	HBM/NMA (40:60)	41.3	11.2	1.31	10.8	1.31
7	–/NMA	0	6.9	1.52	7.3	1.41
8	HBM/NME (95:5)	96.3	6.3	1.46	6.6	1.41
9	HBM/NME (90:10)	90	10.1	1.29	10.3	1.26
10	HBM/NME (85:15)	86.5	9.6	1.32	9.7	1.28
11	HBM/NME (80:20)	80.5	11.1	1.24	9.7	1.29
12	–/NME	0	11.2	1.31	10.8	1.31
13	HBM/NMD (95:5)	94.8	6.9	1.40	9.9	1.39
14	HBM/NMD (90:10)	89.5	10.2	1.36	10.7	1.31
15	HBM/NMD (85:15)	85.3	6.0	1.42	8.8	1.42
16	HBM/NMD (80:20)	78	9.8	1.32	9.8	1.31
17	–/NMD	0	14.6	1.29	13.4	1.32

[a] Polymerization conditions: solvent, dichloromethane; total volume, 30 mL; room temperature; reaction time, 120 min, [monomer]:[**G1**], 300:1; [b] Molar ratio of HBM and comonomer; [c] Determined by ^{1}H NMR. [d] Number-average molecular weight and molecular weight distribution determined by GPC using monodisperse polystyrene standards; M_n, number-average molecular weight; *PDI*, polydispersity index; HBM, *exo*-1,4,4a,9,9a,10-hexahydro-9,10(1′,2′)-benzeno-l,4-methanoanthracene; comonomers: NMA, 5-norbornene-2-yl methylacetate; NME, 5-norbornene-2-yl methyl 2-ethylhexanoate; NMD, 5-norbornene-2-yl methyldodecanoate.

The content of HBM in the copolymers can be calculated by ^{1}H NMR spectra, and the experiment values were consistent with the theoretical ones. A typical ^{1}H NMR spectrum for HBM/NMA copolymer is shown in Figure 1A (entry 2, Table 1, CD₂Cl₂ at 25 °C). The resonances at δ 3.8–4.3 ppm were assigned to the two protons of benzal and methylene, which directly connected norbornene skeleton, and protons of benzene ring in HBM were detected at 6.5–7.2 ppm. The HBM incorporations of the copolymers were calculated from the relative intensities of these protons using the equation:

$$\text{HBM (mol\%)} = (I_{6.5–7.2}/(4 \times I_{3.8–4.3})) \times 100\%$$

where $I_{3.8–4.3}$ ppm is the benzal and methylene signals from HBM and comonomer units, respectively; and $I_{6.5–7.2}$ ppm is from benzene ring in HBM unit. The ratio of the signal intensity was 90.8%, close to the theoretical value (90:10), which also supported the point that the feed cyclic olefins can be quantitatively converted into polymers under these conditions. These results clearly indicated that synthesis of various grades COPs is possible by this approach.
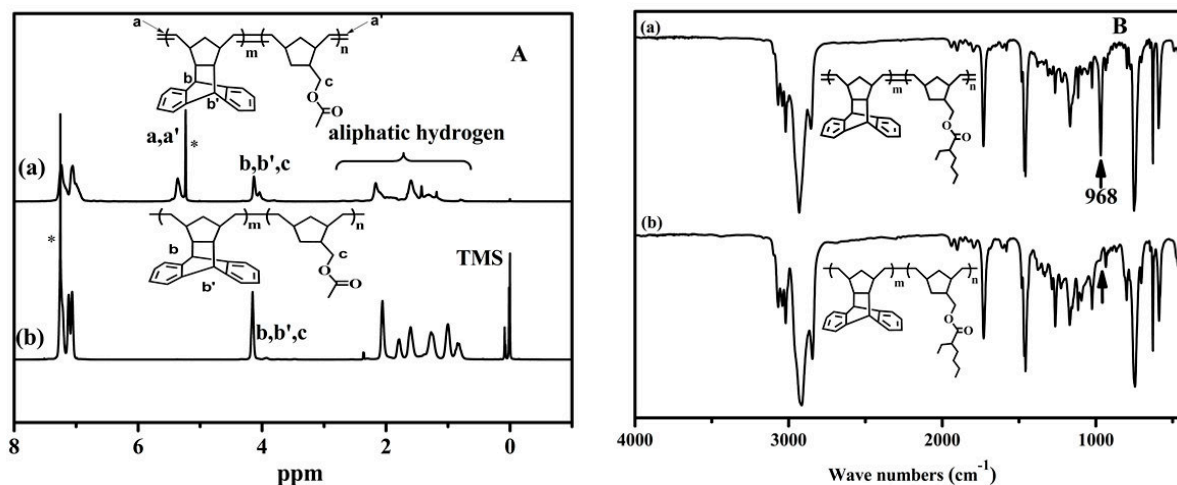
Figure 1. (**A**) ^{1}H NMR spectra of copolymers: (a) poly(HBM-*co*-NMA)(90:10), * signals from CD$_2$Cl$_2$, and (b) corresponding hydrogenated copolymer, * signals from CDCl$_3$; and (**B**) FT-IR spectra of copolymers: (a) poly(HBM-*co*-NME)(85:15), and (b) corresponding hydrogenated copolymer.

The reactivity ratios of HBM and comonomers were estimated by the classical Fineman–Ross method, which were calculated from values of the monomer feed ratio and the analyzed copolymer compositions (see Figures A2–A4 and Tables A1–A3 in Appendix) [44]. For the copolymerization of HBM and NMA, the monomer reactivity ratios (r) were determined to be $r_{HBM} = 1.65$ and $r_{NMA} = 0.59$ (Figure A2 and Table A2 in Appendix). This result indicates that HBM is more reactive than NMA, and the obtained copolymers are a kind of gradient copolymers [45]. The high reactivity of HBM was possibly attributed to high ring strain. Furthermore, the ester group of NMA, especially the *endo*-isomer, may coordinate the active center, which decreased the reactivity of comonomer [46–49]. The same method proved that copolymers of HBM with NME or NMD are also gradient ones (the value $r_{HBM} = 1.58$, $r_{NME} = 0.52$, and $r_{HBM} = 1.37$, $r_{NMD} = 0.7$) (see Figures A3,A4 and Tables A2,A3 in Appendix).

Hydrogenation of the double bonds in main chain of ROMP products was helpful for improving the materials' tolerance towards heat and light. The effective hydrogenation of these copolymers was performed with excess toluenesulfonyl hydrazide. Complete hydrogenation can be confirmed via the disappearance of the signals assigned to the olefinic protons in main chain at 5.0–6.0 ppm in ^{1}H NMR spectrum (Figure 1A,b). The FT-IR spectra of selected copolymers before and after hydrogenation are shown in Figure 1B; the quite clear absorption peak at 968 cm^{-1} is assigned to the out of plane C–H ring bending vibration (Figure 1B,a). However, no absorptions are observed after hydrogenation, which further confirm the complete hydrogenation (Figure 1B,b).

3.2. Thermal Properties of COPs

The glass transition temperatures (T_g) of these obtained polymers were examined by DSC analyses. The typical DSC curves of homopolymers of comonomers are shown in Figure A5 (in Appendix). The T_g decreased substantially after hydrogenation. After hydrogenation, the double bond was replaced by single bond and the flexibility of the polymer chain increased, resulting in lower T_g of the polymer. For example, the T_g value of poly(NMA) (22.4 °C) is 9 °C higher than that of the corresponding

hydrogenated polymer H-poly(NMA) (13.7 °C). Additionally, poly(NMA) exhibit substantially higher T_g values as compared with poly(NME), both before and after hydrogenation. For the hydrogenated homo-polymers, the T_g value of H-poly(NMA) (13.7 °C) is higher by 48 °C than that of poly(NME) (−34.4 °C). This result seems to arise mainly from the reduced flexible side chain of poly(NMA). It is noteworthy that a melting temperature (−18.2 °C) was observed in the DSC curve of poly(NMD) because the long alkyl side chain led to side chain crystallization.
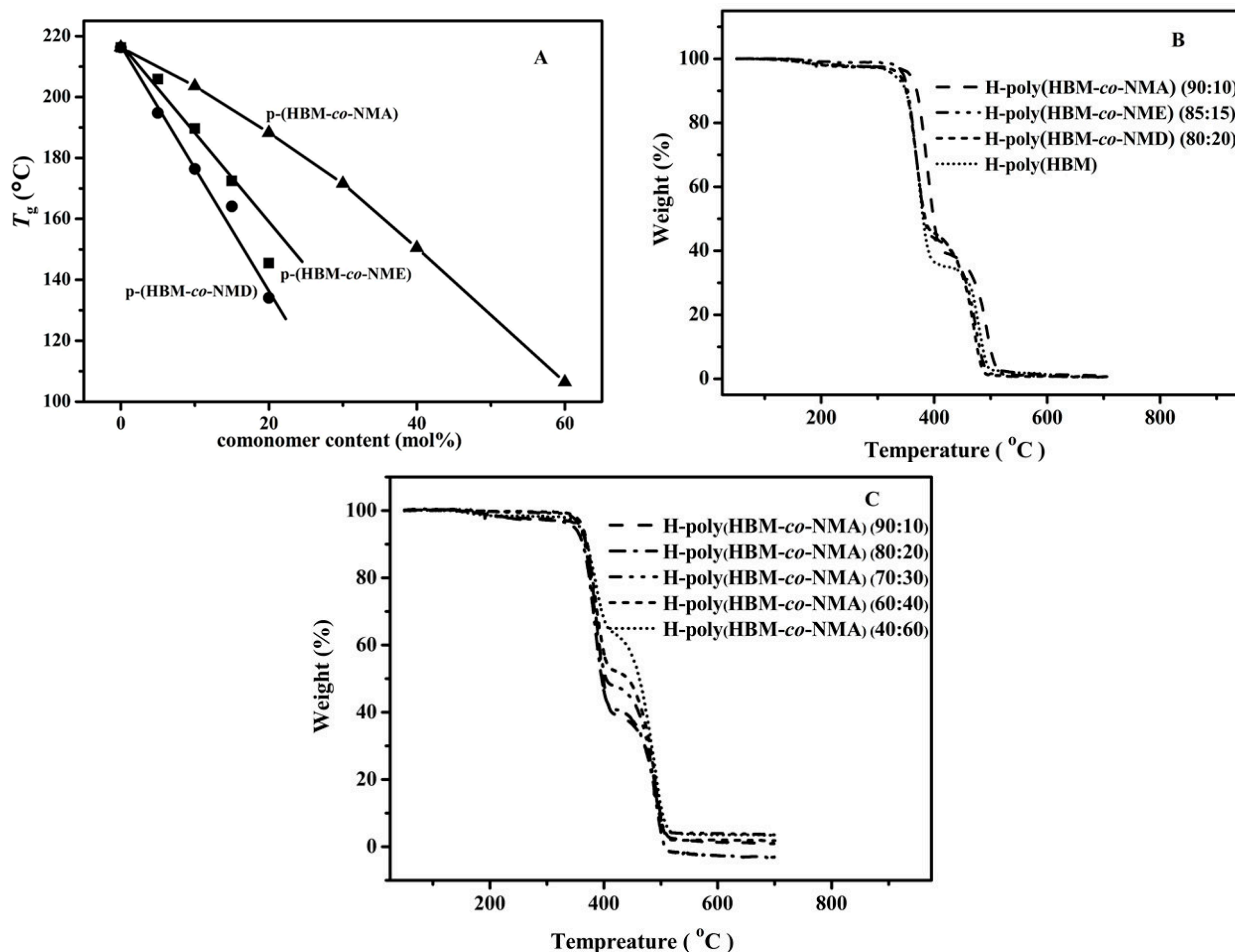

Figure 2. (**A**) plots of T_g of the copolymer *vs.* comonomers incorporation; (**B**) TGA curves of the copolymers of HBM with different comonomers in N₂; (**C**) TGA curves of the copolymers of HBM with NMA in N₂.

As expected, all the hydrogenated copolymers were amorphous, which only exhibited apparent T_g without any melting temperatures (see Figures A6–A8 in Appendix). With increase of the comonomer incorporation, the T_g decreased linearly, as shown in Figure 2A. Interestingly, the H-poly(HBM-*co*-NME) copolymer exhibited the similar T_g values (NME 19.5 mol%, T_g 145.5 °C, entry 10, Table 2) to H-poly(HBM-*co*-NMD) copolymer (NMD 22.0 mol%, T_g 134.1 °C, entry 14, Table 2), whereas H-poly(HBM-*co*-NMA) copolymer exhibited significantly higher T_g (NMA 18.2 mol %, T_g 188.3 °C, entry 3, Table 2) at the same level of comonomer incorporation. The differences became more significant with the increase of the comonomer incorporation. When the content of NMA in copolymer was 40 mol%, the T_g still remained above 150 °C. The results indicated that a wide range of flexible comonomers

(0–40 mol%) incorporation lead to different T_g values in a broad range (220–150 °C). Moreover, all the lines showed good correlation so that various grades of heat-resistant COPs can be obtained predictably by deliberate modulation of the composition of copolymers.

The thermal stability of the obtained copolymers was investigated by TGA. The typical measurement curves are shown in Figure 2B. All copolymers are thermally stable below 350 °C in nitrogen and exhibit two similar thermal decomposition stages above this temperature. The first stage degradation (350–400 °C) was attributed to decomposition of retro Diels–Alder reaction forming anthracene. The second degradation stage (400–500 °C) corresponded to degradation of copolymer structure in main chain. The thermal decomposition stages of H-poly(HBM) were similar to those of the copolymers, which indicated that comonomer incorporation showed little effect on thermal stability of the copolymers. Figure 2C showed the TGA curves of H-poly(HBM-*co*-NMA) copolymers at different levels of NMA. With increase in the comonomer content, the weight loss of the first decomposition stage decreased, which was consistent with the weight occupancy of benzene ring. Meanwhile, the copolymers also showed very similar thermal decomposition behavior in air and in nitrogen (see Figure A9 in Appendix).

3.3. Transparency of Cyclic Olefin Copolymer

Since the molecular weights values of the copolymers seemed to be high enough to form self-standing films, we tried to prepare the copolymer films by casting the tetrachloroethane solutions of the copolymers. To our delight, the self-standing transparent films with a thickness of 80–140 μm were successfully obtained for all these copolymers. The UV-vis measurement indicates that the COPs were always transparency irrelevant to the content and type of comonomers and the transmittance of the COPs was higher than 85% (Figure 3A).
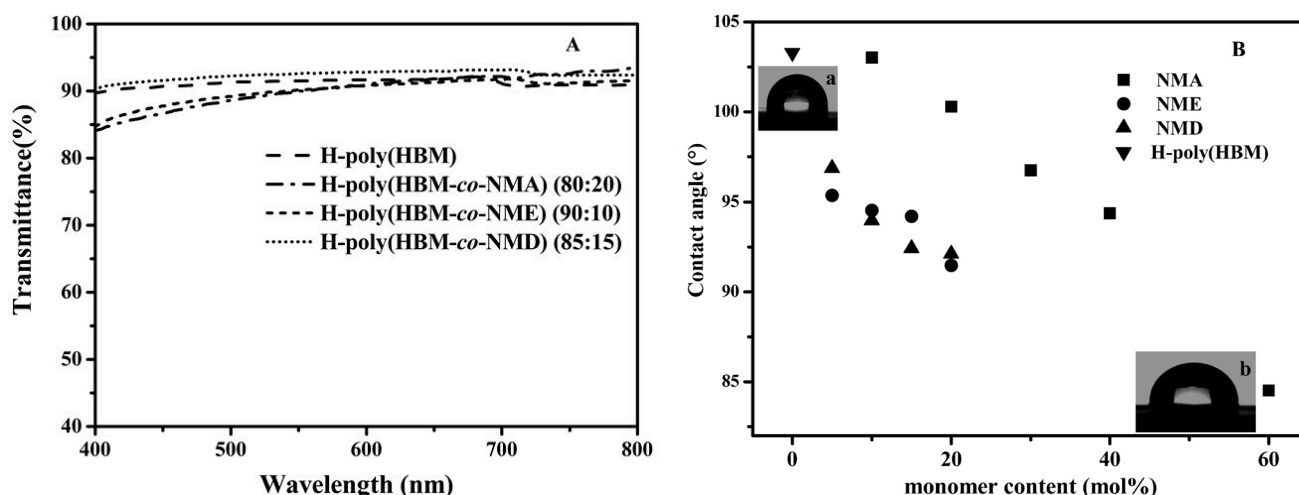

Figure 3. (**A**) Transparency of self-standing COPs films and (**B**) the water contact angle of copolymers (a, H-poly(HBM); b, H-poly(HBM-*co*-NMA) (40:60)).

3.4. Hydrophilicity of Cyclic Olefin Copolymer

The lack of polar groups in COPs has limited their application properties. Because of the ester groups in the comonomers, the resultant copolymers in this work should exhibit some hydrophilic properties. The water contact angles (WCA) of the copolymer films were measured to assess the hydrophilic

properties of the COPs and the typical results were shown in Figure 3B. The contact angle varied in inverse proportion to the ester groups' content in the copolymer (103°–84° in 10–60 mol% of NMA in the copolymers). It was speculated that the contact angle of H-poly(HBM-*co*-NMA) copolymer is smaller than the other copolymers, because short alkyl side chain (methyl) of NMA may make the oxygen more easily exposed on the surface of polymer, resulting in the increase of the polarity of the copolymer. However, it turned out that the result was not consistent with this speculation. As we can see from Figure 3B, the H-poly(HBM-*co*-NMA) copolymers showed higher contact angles than the H-poly(HBM-*co*-NME) and H-poly(HBM-*co*-NMD) ones; namely, the polarity of the H-poly(HBM-*co*-NMA) copolymers was smaller than the others under the same comonomer incorporation. It was possible that hydrophobic long alkyl side chain in H-poly(HBM-*co*-NME) and H-poly(HBM-*co*-NMD) copolymers caused its rearrangement and extended toward the inside of polymer membrane, which exposed the ester group on the surface of the polymer membrane. However, for H-poly(HBM-*co*-NMA) copolymer, hydrophobic short alkyl side chain (methyl) randomly distributed on the surface of polymer membrane causing low oxygen concentration on the surface of polymer membrane.

In order to prove this assumption, X-ray photoelectron spectroscopy (XPS) studies were conducted to evaluate the oxygen concentration on the surface of copolymer films. The results showed that the oxygen concentration in H-poly(HBM-*co*-NMA) (20 mol%) copolymers surface was indeed lower than H-poly(HBM-*co*-NMD) (20 mol%) (see Figure A10 in Appendix), which was consistent with the higher WCA of poly(HBM-*co*-NMA)(Figure 3B). The oxygen concentration increased and the WCA decreased correspondingly with the increase of the content of NMA in the copolymer.

3.5. Mechanical Properties of Cyclic Olefin Copolymer

In this work, the COPs with higher flexible comonomer incorporation even display higher T_g, which may be promising for improving mechanical performance without sacrificing high T_g of the COPs. Therefore, the tensile test was further conducted to verify their mechanical performance. The stress–strain behaviors were measured under the similar conditions as a previous report [15]. The typical results are provided in Table 2, for the HBM homopolymer with T_g of 216.3 °C, a strain at break of 1.9% was observed (entry 1, Table 2). With increase of the content of comonomer, the strain at break (ε_b) of the copolymer increased gradually and the tensile strength (σ) and tensile modulus (E) decreased gradually (entries 2–6, 7–10, 1–14, Table 2). The enhanced flexibility can be clearly explained by the increased chain entanglement as copolymers contain higher amount of flexible comonomers units. Although the σ and the E value decreased, ε_b gradually increased from 2.8% to 9.7% as the content of NMA increased. All copolymers were similar flexible at the same level of comonomer incorporation. Meanwhile, all the copolymers exhibited higher T_g, more than 150 °C, except that NMA incorporation was 60 mol%, which indicated the resulted copolymers possess both high T_g and improved mechanical performance.

Table 2. Tensile Properties of the COPs films [a].

Entry	[HBM]:[M] [b]	HBM mol%	σ (MPa) [b]	E (MPa) [c]	ε_b (%) [d]	T_g (°C)
1	–/HBM	100	28.8	1,910	1.9	216.3
2	HBM/NMA (90:10)	90.8	24.4	1,193	2.8	203.6
3	HBM/NMA (80:20)	81.8	23.6	1,140	3.7	188.3
4	HBM/NMA (70:30)	72.5	23.4	1,102	4.5	171.6
5	HBM/NMA (60:40)	62.5	21.7	1,042	6.9	150.5
6	HBM/NMA (40:60)	41.3	17.7	1,190	9.7	106.4
7	HBM/NME (95:5)	96.5	22.4	1,580	1.7	205.9
8	HBM/NME (90:10)	90	22.0	1,350	1.8	189.7
9	HBM/NME (85:15)	86.5	20.4	1,320	2	172.5
10	HBM/NME (80:20)	80.5	18.8	1,170	2.8	145.5
11	HBM/NMD (95:5)	94.8	30.8	1,630	2.1	194.8
12	HBM/NMD (90:10)	89.5	28.5	1,557	2.8	176.4
13	HBM/NMD (85:15)	85.3	25.7	1,258	2.9	164.1
14	HBM/NMD (80:20)	78	19.2	1,077	3.2	134.1

[a] Samples were prepared via solution casting and were measured at cross-head rate of 5 mm/min; [b] Tensile strength; [c] Tensile modulus; and [d] Strain at break.

4. Conclusions

Using the Grubbs first generation catalyst (**G1**), a series of COPs containing ester groups have been synthesized via ROMP and subsequent hydrogenation. ^{1}H NMR spectra and FT-IR spectroscopy reveal the copolymers were completely hydrogenated. The T_g values of the resulting copolymers could be modulated by changing the comonomer content. The presence of ester groups in the copolymer structures effectively adjusted the hydrophilicity of copolymers. Based on the thermal stability and certain polarity, improved mechanical performance, associated with excellent transparency and good film forming ability, is expected to broaden the applicability of COPs and demonstrate their broad range of achievable polymer properties.

Appendix

The comonomers used were synthesized via an acylation reaction of 5-norbornene-2-methanol with different fatty acyl chloride in the presence of triethylamine according to a literature procedure [50,51].

A1. Synthesis of 5-Norbornene-2-yl Methyl acetate (NMA)

A 1.0-mol 5-norbornene-2-methanol, 1.0-mol triethylamine and 30 mL dichloromethane mixture was placed in a dried, 500-mL, branched, round-bottomed flask equipped with a magnetic stirrer, a dropping funnel. When the device was placed in the ice water bath, acetylchloride 1.5 mol was added dropwise under stirring. The reaction mixture was under constant stirring for 15 h. Then, 100 mL water was poured into the solution. The mixture was extracted with water, saturated sodium carbonate, and sodium chloride solution. The organic layer was separated, and dried with anhydrous sodium sulfate. Finally, the solution was filtered and removed anhydrous sodium sulfate. The yield of NMA: 93.8%. ^{1}H NMR (399.65 MHz, CDCl₃), δ (ppm) (Scheme A1): 6.15 (dd, J = 3.0 and 5.7 Hz, 0.67H, H$_{endo1}$), 6.12–6.04 (m, 0.66H, H$_{exo1}$

and H$_{exo2}$), 5.94 (dd, *J* = 2.9 and 5.7 Hz, 0.67H, H$_{endo2}$), 3.91–4.13 (m, 0.67H, H$_{exo8}$), 3.6–3.83 (m, 1.33H, H$_{endo8}$), 2.88 (s, 0.67H, H$_{endo3}$), 2.82 (d, *J* = 8.3 Hz, 1H, H$_{endo4}$ and H$_{exo3}$), 2.70 (s, 0.33H, H$_{exo4}$), 2.31–2.47 (m, 0.67H, H$_{endo5}$), 1.93–2.17 (m, 3H, H$_{10}$), 1.79–1.91 (m, 0.67H, H$_{endo6a}$), 1.67–1.77 (m, 0.33H, H$_{exo5}$), 1.40–1.50 (m, 0.67H, H$_{endo6b}$), 1.32–1.40 (m, 1.67H, H$_{endo7a}$, H$_{exo7a}$ and H$_{endo7b}$), 1.12–1.2 (m, 0.33H, H$_{exo6a}$), 0.57 (dd, *J* = 2.6 and 4.4 Hz, 0.33H, H$_{exo7b}$), 0.54 (dd, *J* = 2.6 and 4.4 Hz, 0.33H, H$_{exo6b}$). ^{13}C NMR (100.40 MHz, CDCl$_3$) δ (ppm): 170.99, 170.91, 137.56, 136.91, 136.23, 132.17, 68.54, 67.86, 49.52, 42.24, 37.83, 29.04, 20.96, and 20.94.

A2. Synthesis of 5-Norbornene-2-yl Methyl 2-Ethylhexanoate (NME)

(a) A 0.25 mol of isocaprylic acid was placed in a dried, 500-mL, three-necked, round-bottomed flask equipped with a magnetic stirrer, a dropping funnel, a water condenser and a thermometer. On the top of the condenser, an exit tube with a gas-absorption trap was attached to remove the reaction of hydrogen chloride. When the solution was heated to 60 °C, thionyl chloride 0.5 mol was added dropwise under stirring. The reaction mixture was heated and refluxed on a steam bath, until no more hydrogen chloride evolved. Excess thionyl chloride was removed by distillation at atmospheric pressure. Then, isocaprylic acid chloride was distilled off under reduced pressure. The yield of the product: 95%.

(b) NME comonomer was synthesized applying a similar procedure as described for the preparation of NMA. The yield of NME: 90.5%.

^{1}H NMR (399.65 MHz, CDCl$_3$), δ (ppm) (Scheme A1): the intensity of 0.5–2.25 corresponds to 19.33H (m, H$_{exo5}$, H$_{endo6a}$, H$_{exo6a}$, H$_{endo6b}$, H$_{exo6b}$, H$_{endo7a}$, H$_{exo7a}$, H$_{endo7b}$, H$_{exo7b}$, and H$_{10-16}$). ^{13}C NMR (100.40 MHz, CDCl$_3$) δ (ppm): 176.28, 176.18, 137.43, 136.79, 136.12, 132.07, 68.08, 67.34, 43.85, 42.16, 41.55, 38.03, 37.83, 31.78, 28.90, 22.56, 13.86, and 11.80.

A3. Synthesis of 5-Norbornene-2-yl Methyldodecanoate (NMD)

NMD comonomer was synthesized via a similar procedure as described for the preparation of NME starting with dodecanoic acid. The yield of products: (a) 98%; (b) 94.6%.

^{1}H NMR (399.65 MHz, CDCl$_3$), δ (ppm) (Scheme A1): the intensity of 0.54–2.32 corresponds to 27.33H (m, H$_{exo5}$, H$_{endo6a}$, H$_{exo6a}$, H$_{endo6b}$, H$_{exo6b}$, H$_{endo7a}$, H$_{exo7a}$, H$_{endo7b}$, H$_{exo7b}$, and H$_{10-20}$). ^{13}C NMR (100.40 MHz, CDCl$_3$) δ (ppm): 173.80, 173.70, 137.47, 136.84, 136.18, 132.13, 68.28, 67.59, 49.33, 44.92, 43.65, 42.18, 41.56, 37.99, 37.83, 34.37, 31.88, 29.57, 29.45, 29.30, 29.25, 29.14, 28.96, 25.05, 25.02, 22.65, and 14.05.
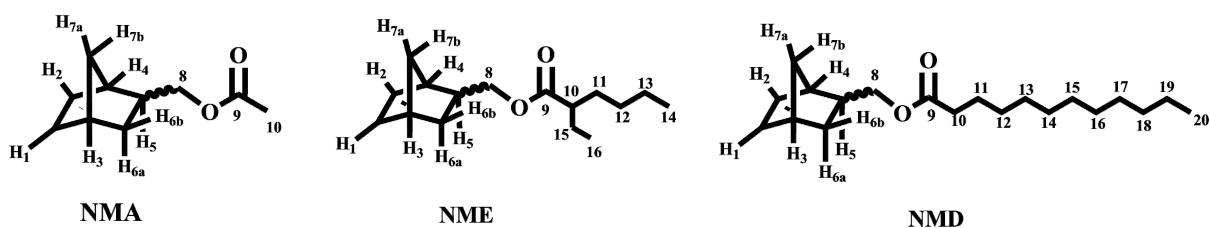
Scheme A1. Structure of *endo/exo*-isomer (2:1) of monomers (NMA, comonomers (5-norbornene-2-yl methylacetate; NME, 5-norbornene-2-yl methyl 2-ethylhexanoate; NMD, 5-norbornene-2-yl methyldodecanoate).
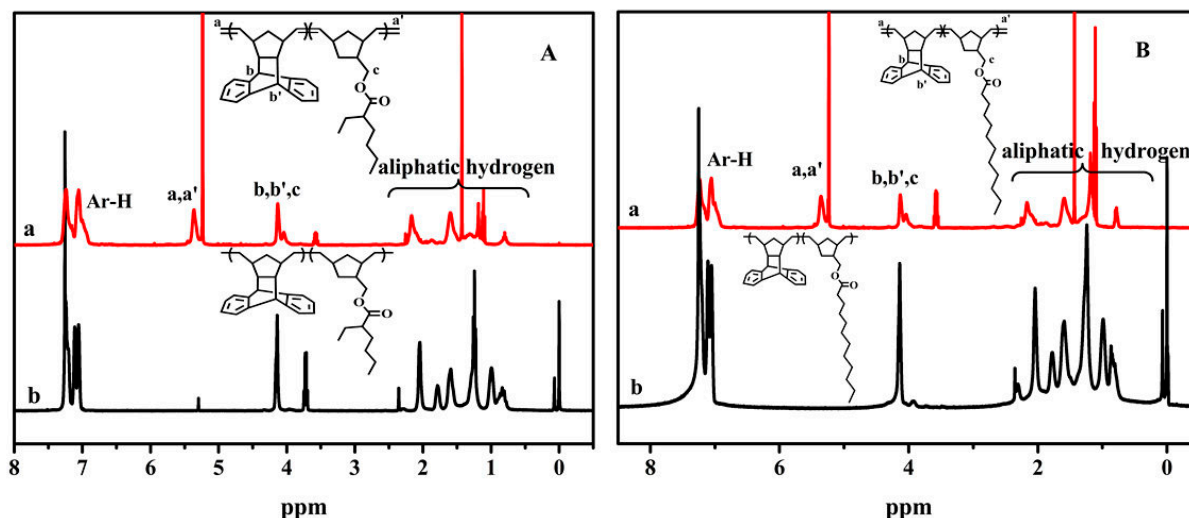
A4. The ^{1}H NMR Spectra for the Copolymers

Figure A1. The ^{1}H NMR spectra for the copolymers. (**A**), (a) poly(HBM-co-NME) (95:5) in CD$_2$Cl$_2$, (b) corresponding hydrogenated copolymer in CDCl$_3$; (**B**), poly(HBM-*co*-NMD) (85:15) in CD$_2$Cl$_2$, and (b) corresponding hydrogenated copolymer in CDCl$_3$.

A5. Reactivity Ratios of Copolymerization

Copolymerization of HBM and NMA using the Grubbs first generation catalyst Ru(CHPh)(Cl)$_2$(PCy$_3$)$_2$ (Cy = cyclohexyl, **G1**) was performed in dichloromethane at room temperature with various monomer feed compositions (<10% conversion). The reactivity ratios can be obtained by using Equation (A1) (the Fineman–Ross method), for which the reactivity ratio of NMA (r_{NMA}) is the negative value of the slope and reactivity ratio of HBM (rHBM) is the intercept.

$$(f-1)/F = -r_{NMA} \times f/F^2 + r_{HBM} \tag{A1}$$

where *f* refer to the ratio of NMA and HBM compositions in copolymers, respectively; *F* refer to the ratio of the feed compositions of NMA and HBM monomers. The values of various parameters for calculating reactivity ratios of NMA and HBM are summarized in Table A1. Figure A1 shows the plot of (*f*−1)/*F versus f/F*^{2}. From data fitting by the least-squares regression, the obtained reactivity ratios of HBM (*r*HBM) and NMA (*r*NMA) are 1.65 and 0.59, respectively. The value $r_{HBM} \times r_{NMA} = 0.96$, being less than 1, shows that the copolymers synthesized using **G1** are random ones.

Table A1. Various parameters for calculating reactivity ratios of *exo*-1,4,4a,9,9a,10-hexahydro-9,10(1′,2′)-benzeno-l,4-methanoanthracene (HBM) and 5-Norbornene-2-yl Methylacetate (NMA).

Entry [a]	M_{NMA}	M_{HBM}	m_{NMA}	m_{HBM}	f [b]	F [c]	f/F^2	$(f-1)/F$
1	0.4	0.6	0.285	0.715	0.399	0.667	0.897	−0.901
2	0.6	0.4	0.483	0.518	0.932	1.5	0.414	−0.045
3	0.7	0.3	0.563	0.438	1.286	2.333	0.236	0.123
4	0.9	0.1	0.848	0.153	5.557	9	0.069	0.506

[a] Copolymers obtained at low conversion (<10%) from different monomer feed compositions; [b] f, m_{NMA}/m_{HBM}, and m_{NMA} and m_{HBM} refer to NMA and HBM compositions in copolymers, respectively; [c] F, M_{NMA}/M_{HBM}, and M_{NMA} and M_{HBM} refer to the feed compositions of NMA and HBM monomers, respectively.
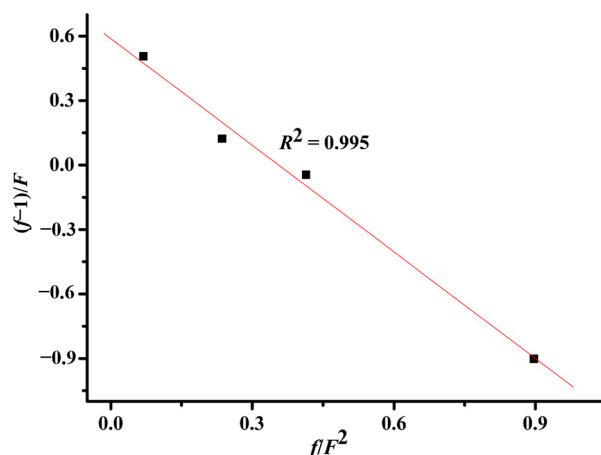
Figure A2. Plot of (f-1)/F *versus f/F^2* with least-squares regression line for HBM and NMA copolymerization.

Figure A2 shows the plot of ($f-1$)/F *versus f/F^2*. From data fitting by the least-squares regression, the obtained reactivity ratios of HBM (rHBM) and NME (rNME) are 1.58 and 0.52, respectively. The value $r_{HBM} \times r_{NME} = 0.82$, being less than 1, shows that the copolymers synthesized using **G1** are random ones.

Table A2. Various parameters for calculating reactivity ratios of HBM and 5-Norbornene-2-yl Methyl 2-Ethylhexanoate (NME).

Entry [a]	M_{NME}	M_{HBM}	m_{NME}	m_{HBM}	f [b]	F [c]	f/F^2	($f-1$)/F
1	0.300	0.700	0.200	0.800	0.250	0.429	1.358	−1.748
2	0.400	0.600	0.298	0.703	0.423	0.667	0.951	−0.865
3	0.500	0.500	0.383	0.618	0.619	1.000	0.619	−0.381
4	0.700	0.300	0.573	0.428	1.339	2.333	0.246	0.145
5	0.900	0.100	0.805	0.195	4.128	9.000	0.051	0.346

[a] Copolymers obtained at low conversion (<10%) from different monomer feed compositions; [b] f, m_{NME}/m_{HBM}, and mNME and mHBM refer to NME and HBM compositions in copolymers, respectively; [c] F, M_{NME}/M_{HBM}, and M_{NME} and M_{HBM} refer to the feed compositions of NME and HBM monomers, respectively.

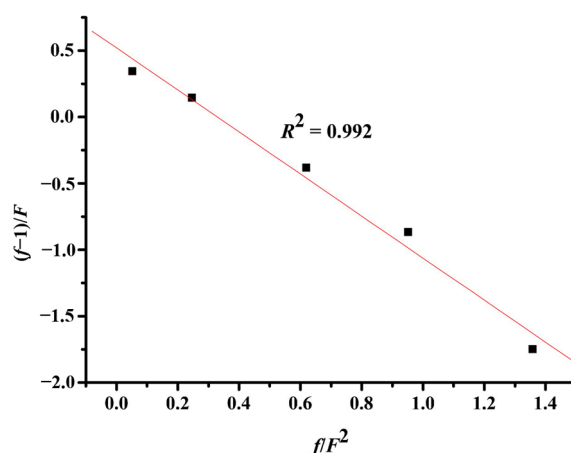**Figure A3.** Plot of ($f-1$)/F *versus f/F^2* with least-squares regression line for HBM and NME copolymerization.

Figure A3 shows the plot of $(f-1)/F$ *versus* f/F^2. From data fitting by the least-squares regression, the obtained reactivity ratios of HBM (rHBM) and NME (rNME) are 1.37 and 0.7, respectively. The value $r_{HBM} \times r_{NMD} = 0.96$, being less than 1, shows that the copolymers synthesized using **G1** are random ones.

Table A3. Various parameters for calculating reactivity ratios of HBM and 5-Norbornene-2-yl Methyldodecanoate (NMD).

Entry [a]	M_{NME}	M_{HBM}	m_{NME}	m_{HBM}	f [b]	F [c]	f/F^2	$(f-1)/F$
1	0.400	0.600	0.320	0.680	0.471	0.667	1.059	−0.794
2	0.500	0.500	0.427	0.573	0.747	1.000	0.747	−0.253
3	0.700	0.300	0.623	0.377	1.649	2.333	0.303	0.278
4	0.900	0.100	0.863	0.137	6.273	9.000	0.077	0.586

[a] Copolymers obtained at low conversion (<10%) from different monomer feed compositions; [b] f, m_{NMD}/m_{HBM}, and m_{NMD} and m_{HBM} refer to NMD and HBM compositions in copolymers, respectively; [c] F, M_{NMD}/M_{HBM}, and M_{NMD} and M_{HBM} refer to the feed compositions of NMD and HBM monomers, respectively.
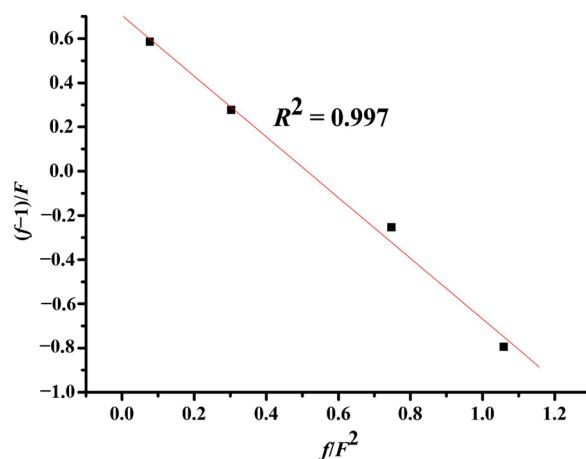

Figure A4. Plot of $(f-1)/F$ *versus* f/F^2 with least-squares regression line for HBM and NMD copolymerization.

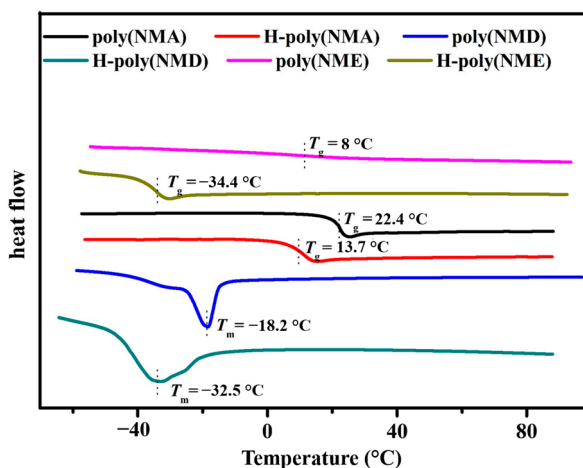## A6. Thermal Properties of COPs

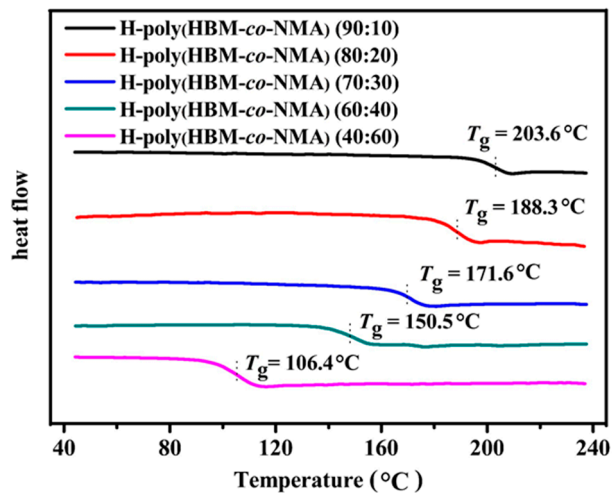**Figure A5.** Differential scanning calorimetry (DSC) curves of homopolymers before and after hydrogenation.

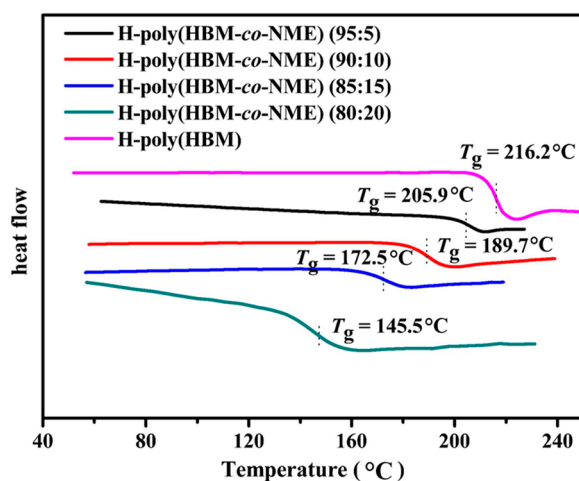**Figure A6.** DSC curves of copolymers of HBM and NMA.

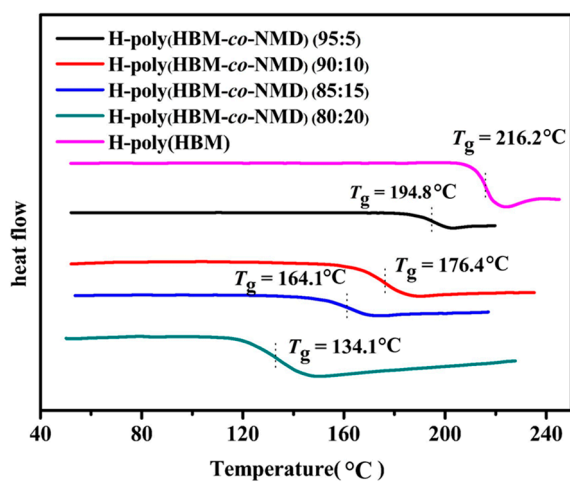**Figure A7.** DSC curves of copolymers of HBM and NME.

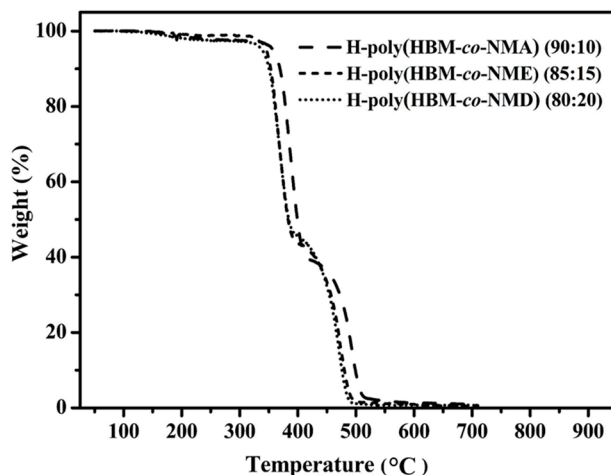**Figure A8.** DSC curves of copolymers of HBM and NMD.

Figure A9. Thermogravimetric analyses of compolymers of HBM with different comonomers in air.
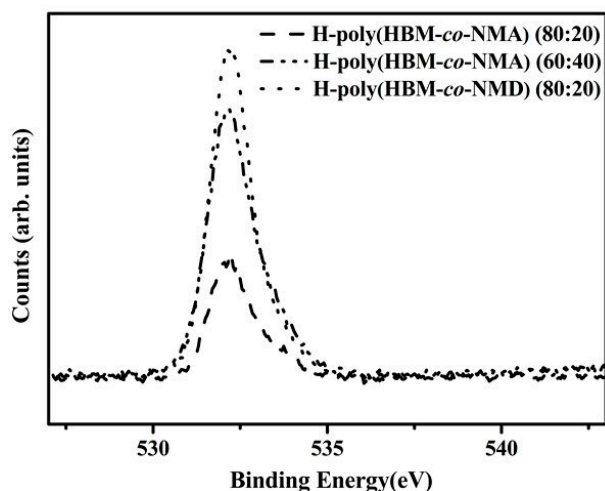
A7. X-ray Photoelectron Spectroscopy (XPS) Test

Figure A10. O 1s X-ray Photoelectron Spectroscopy spectra of copolymers.

Acknowledgments

Author Contributions

All authors tried their best to contribute effectively to perform and analyze this experimental work. They all participated to the writing of the present manuscript. Jing Cui performed the overall experimental work as a Ph.D Student in Tianjin University, China. Jixing Yang participated in analysis of structural data. The settings up of the experimental protocols as well as the interpretation of the obtained results were performed under the supervision of Yanguo Li and Yuesheng Li.

Conflicts of Interest

The authors declare no conflict of interest.

References

1. Khanarian, G. Optical properties of cyclic olefin copolymers. *Opt. Eng.* **2001**, *40*, 1024–1029.
2. Mol, J.C. Industrial applications of olefin metathesis. *J. Mol. Catal. A* **2004**, *213*, 39–45.
3. Nunes, P.; Ohlsson, P.; Ordeig, O.; Kutter, J. Cyclic olefin polymers: Emerging materials for lab-on-a-chip applications. *Microfluid. Nanofluid.* **2010**, *9*, 145–161.
4. Shin, J.Y.; Park, J.Y.; Liu, C.Y.; He, J.S.; Kim, S.C. Chemical structure and physical properties of cyclic olefin copolymers (IUPAC technical report). *Pure Appl. Chem.* **2005**, *77*, 801–814.
5. Cho, E.S.; Joung, U.G.; Lee, B.Y.; Lee, H.; Park, Y.-W.; Lee, C.H.; Shin, D.M. Syntheses of 2,5-dimethylcyclopentadienyl ansa-zirconocene complexes and their reactivity for ethylene/norbornene copolymerization. *Organometallics* **2004**, *23*, 4693–4699.
6. Li, X.; Baldamus, J.; Hou, Z. Alternating ethylene–norbornene copolymerization catalyzed by cationic half-sandwich scandium complexes. *Angew. Chem. Int. Ed.* **2005**, *44*, 962–965.
7. Li, X.; Hou, Z. Organometallic catalysts for copolymerization of cyclic olefins. *Coord. Chem. Rev.* **2008**, *252*, 1842–1869.
8. McKnight, A.L.; Waymouth, R.M. Ethylene/norbornene copolymerizations with titanium CpA catalysts. *Macromolecules* **1999**, *32*, 2816–2825.
9. Na, S.J.; Wu, C.J.; Yoo, J.; Kim, B.E.; Lee, B.Y. Copolymerization of 5,6-dihydro-dicyclopentadiene and ethylene. *Macromolecules* **2008**, *41*, 4055–4057.
10. Nomura, K.; Wang, W.; Fujiki, M.; Liu, J. Notable norbornene (NBE) incorporation in ethylene-NBE copolymerization catalysed by nonbridged half-titanocenes: Better correlation between NBE incorporation and coordination energy. *Chem. Commun.* **2006**, 2659–2661.
11. Ruchatz, D.; Fink, G. Ethene−Norbornene Copolymerization Using homogenous metallocene and half-sandwich catalysts: Kinetics and relationships between catalyst structure and polymer structure. 2. Comparative study of different metallocene- and half-sandwich/methylaluminoxane catalysts and analysis of the copolymers by ^{13}C nuclear magnetic resonance spectroscopy. *Macromolecules* **1998**, *31*, 4674–4680.
12. Ruchatz, D.; Fink, G. Ethene-norbornene copolymerization using homogenous metallocene and half-sandwich catalysts: Kinetics and relationships between catalyst structure and polymer structure. 1. Kinetics of the ethene-norbornene copolymerization using the [(isopropylidene)(η5-inden-1-ylidene-η5-cyclopentadienyl)]zirconium dichloride/methylaluminoxane catalyst. *Macromolecules* **1998**, *31*, 4669–4673.
13. Ruchatz, D.; Fink, G. Ethene-norbornene copolymerization with homogeneous metallocene and half-sandwich catalysts: Kinetics and relationships between catalyst structure and polymer structure. 4. Development of molecular weights. *Macromolecules* **1998**, *31*, 4684–4686.
14. Tritto, I.; Boggioni, L.; Ferro, D.R. Metallocene catalyzed ethene- and propene co-norbornene polymerization: Mechanisms from a detailed microstructural analysis. *Coord. Chem. Rev.* **2006**, *250*, 212–241.

15. Yu, S.T.; Na, S.J.; Lim, T.S.; Lee, B.Y. Preparation of a bulky cycloolefin/ethylene copolymer and its tensile properties. *Macromolecules* **2010**, *43*, 725–730.

16. Liu, M.O.; Lin, H.F.; Yang, M.C.; Lai, M.J.; Chang, C.C.; Shiao, P.L.; Chen, I.M.; Chen, J.Y. Thermal, dynamic mechanical and rheological properties of metallocene-catalyzed cycloolefin copolymers (mCOCs) with high glass transition temperature. *Mater. Lett.* **2007**, *61*, 457–462.

17. Ban, H.T.; Shigeta, M.; Nagamune, T.; Uejima, M. Synthesis of cyclo-olefin copolymer latexes and their carbon nanotube composite nanoparticles. *J. Polym. Sci. Part A* **2013**, *51*, 4584–4591.

18. Kim, J.; Wu, C.J.; Kim, W.J.; Kim, J.; Lee, H.; Kim, J.D. Ring-opening metathesis polymerization of tetracyclododecene using various catalyst systems. *J. Appl. Polym. Sci.* **2010**, *116*, 479–485.

19. Kwon, O.J.; Huyen Thanh, V.; Lee, S.B.; Kim, T.K.; Kim, H.S.; Lee, H. Ring-opening metathesis polymerization and hydrogenation of ethyl-substituted tetracyclododecene. *Bull. Korean Chem. Soc.* **2011**, *32*, 2737–2742.

20. Lian, W.R.; Wu, H.Y.; Wang, K.L.; Liaw, D.J.; Lee, K.R.; Lai, J.Y. High glass transition and thermally stable polynorbornenes containing fluorescent dipyrene moieties via ring-opening metathesis polymerization. *J. Polym. Sci. Part A* **2011**, *49*, 3673–3680.

21. Okaniwa, M.; Kawashima, N.; Kaizu, M.; Mutsuga, Y. Birefringence control by hydrogen bonding on compatible polymer pair composed of hydrogenated ring-opening polymer and modified polystyrene. *J. Polym. Sci. Part A* **2013**, *51*, 3132–3143.

22. Park, E.S.; Park, J.H.; Jeon, J.; Sung, J.U.; Hwang, W.S.; Lee, B.Y. Ring-opening metathesis polymerization of dicyclopentadiene and tricyclopentadiene. *Macromol. Res.* **2013**, *21*, 114–117.

23. Shiotsuki, M.; Endo, T. Synthesis of hydrocarbon polymers containing bulky dibenzobicyclic moiety by ROMP and their characteristic optical properties. *J. Polym. Sci. Part A* **2014**, *52*, 1392–1400.

24. Widyaya, V.T.; Vo, H.T.; Putra, R.D.D.; Hwang, W.S.; Ahn, B.S.; Lee, H. Preparation and characterization of cycloolefin polymer based on dicyclopentadiene (DCPD) and dimethanooctahydronaphthalene (DMON). *Eur. Polym. J.* **2013**, *49*, 2680–2688.

25. Yamazaki, M. Industrialization and application development of cyclo-olefin polymer. *J. Mol. Catal. A* **2004**, *213*, 81–87.

26. Cai, Z.; Harada, R.; Nakayama, Y.; Shiono, T. Highly active living random copolymerization of norbornene and 1-alkene with ansa-fluorenylamidodimethyltitanium derivative: Substituent effects on fluorenyl ligand. *Macromolecules* **2010**, *43*, 4527–4531.

27. Forsyth, J.F.; Scrivani, T.; Benavente, R.; Marestin, C.; Pereña, J.M. Thermal and dynamic mechanical behavior of ethylene/norbornene copolymers with medium norbornene contents. *J. Appl. Polym. Sci.* **2001**, *82*, 2159–2165.

28. Rische, T.; Waddon, A.J.; Dickinson, L.C.; MacKnight, W.J. Microstructure and morphology of cycloolefin copolymers. *Macromolecules* **1998**, *31*, 1871–1874.

29. Park, H.C.; Kim, A.; Lee, B.Y. Preparation of cycloolefin copolymers of a bulky tricyclo-pentadiene. *J. Polym. Sci. Part A* **2011**, *49*, 938–944.

30. Hong, M.; Yang, G.F.; Long, Y.Y.; Yu, S.; Li, Y.S. Preparation of novel cyclic olefin copolymer with high glass transition temperature. *J. Polym. Sci. Part A* **2013**, *51*, 3144–3152.

31. Hong, M.; Cui, L.; Liu, S.; Li, Y. Synthesis of novel cyclic olefin copolymer (COC) with high performance via effective copolymerization of ethylene with bulky cyclic olefin. *Macromolecules* **2012**, *45*, 5397–5402.

32. Yang, J.X.; Cui, J.; Long, Y.Y.; Li, Y.G.; Li, Y.S. Synthesis of cyclic olefin polymers with high glass transition temperature by ring-opening metathesis copolymerization and subsequent hydrogenation. *J. Polym. Sci. Part A* **2014**, *52*, 2654–2661.

33. Yang, J.X.; Cui, J.; Long, Y.Y.; Li, Y.G.; Li, Y.S. Synthesis of novel cyclic olefin polymers with excellent transparency and high glass-transition temperature via gradient copolymerization of bulky cyclic olefin and cis-cyclooctene. *J. Polym. Sci. Part A* **2014**, *52*, 3240–3249.

34. Slugovc, C.; Demel, S.; Riegler, S.; Hobisch, J.; Stelzer, F. Influence of functional groups on ring opening metathesis polymerisation and polymer properties. *J. Mol. Catal. A* **2004**, *213*, 107–113.

35. Shiono, T.; Sugimoto, M.; Hasan, T.; Cai, Z. Facile synthesis of hydroxy-functionalized cycloolefin copolymer using ω-alkenylaluminium as a comonomer. *Macromol. Chem. Phys.* **2013**, *214*, 2239–2244.

36. Lee, J.W.; Jantasee, S.; Jongsomsjit, B.; Tanaka, R.; Nakayama, Y.; Shiono, T. Copolymerization of norbornene with ω-alkenylaluminum as a precursor comonomer for introduction of carbonyl moieties. *J. Polym. Sci. Part A* **2013**, *51*, 5085–5090.

37. Binder, J.B.; Raines, R.T. Olefin metathesis for chemical biology. *Curr. Opin. Chem. Biol.* **2008**, *12*, 767–773.

38. Leitgeb, A.; Wappel, J.; Slugovc, C. The ROMP toolbox upgraded. *Polymer* **2010**, *51*, 2927–2946.

39. Slugovc, C. The ring opening metathesis polymerisation toolbox. *Macromol. Rapid Commun.* **2004**, *25*, 1283–1297.

40. Sutthasupa, S.; Shiotsuki, M.; Sanda, F. Recent advances in ring-opening metathesis polymerization, and application to synthesis of functional materials. *Polym. J.* **2010**, *42*, 905–915.

41. Trnka, T.M.; Grubbs, R.H. The development of L_2X_2RuCHR olefin metathesis catalysts: An organometallic success story. *Acc. Chem. Res.* **2001**, *34*, 18–29.

42. Schwab, P.; Grubbs, R.H.; Ziller, J.W. Synthesis and applications of $RuCl_2(=CHR')(PR_3)_2$: The influence of the alkylidene moiety on metathesis activity. *J. Am. Chem. Soc.* **1996**, *118*, 100–110.

43. Schwab, P.; France, M.B.; Ziller, J.W.; Grubbs, R.H. A Series of well-defined metathesis catalysts–synthesis of $[RuCl_2(=CHR')(PR_3)_2]$ and its reactions. *Angew. Chem. Int. Ed.* **1995**, *34*, 2039–2041.

44. Tidwell, P.W.; Mortimer, G.A. An improved method of calculating copolymerization reactivity ratios. *J. Polym. Sci. Part A* **1965**, *3*, 369–387.

45. Mayo F.R.; Lewis F.M. Copolymerization. I. A basis for comparing the behavior of monomers in copolymerization; the copolymerization of styrene and methyl methacrylate. *J. Am. Chem. Soc.* **1944**, *66*, 1594–1601.

46. Rule, J.D.; Moore, J.S. ROMP reactivity of endo- and exo-dicyclopentadiene. *Macromolecules* **2002**, *35*, 7878–7882.

47. Sutthasupa, S.; Sanda, F.; Masuda, T. Ring-opening metathesis polymerization of amino acid-functionalized norbornene diamide monomers: Polymerization behavior and chiral recognition ability of the polymers. *Macromol. Chem. Phys.* **2008**, *209*, 930–937.

48. Sutthasupa, S.; Terada, K.; Sanda, F.; Masuda, T. Ring-opening metathesis polymerization of amino acid-functionalized norbornene derivatives. *J. Polym. Sci. Part A* **2006**, *44*, 5337–5343.

49. Sutthasupa, S.; Terada, K.; Sanda, F.; Masuda, T. Ring-opening metathesis polymerization of amino acid-functionalized norbornene diester monomers. *Polymer* **2007**, *48*, 3026–3032.

50. Yang, F.; Li, G.; Xu, N.; Liu, R.; Zhang, S.-M.; Wu, Z.-J. Synthesis and critical micelle concentration of a series of gemini alkylphenol polyoxyethylene nonionic surfactants. *J. Surfact. Deterg.* **2011**, *14*, 339–345.

51. Blanco, J.M.; Fernández, F.; García-Mera, X.; Rodríguez-Borges, J.E. Divergent synthesis of two precursors of 3'-homo-2'-deoxy- and 2'-homo-3'-deoxy-carbocyclic nucleosides. *Tetrahedron* **2002**, *58*, 8843–8849.